A regenerable screen-printed voltammetric Hg(II) ion sensor based on tris-thiourea organic chelating ligand grafted graphene nanomaterial

Suhaila Sapari [a], Nurul Hidayah Abdul Razak [a], Siti Aishah Hasbullah [a], Lee Yook Heng [a,b], Kwok Feng Chong [c], Ling Ling Tan [b,*]

[a] Department of Chemical Sciences, Faculty Science and Technology, Universiti Kebangsaan Malaysia, 43600 UKM Bangi, Selangor, Malaysia
[b] Southeast Asia Disaster Prevention Research Initiative (SEADPRI-UKM), Institute for Environment and Development (LESTARI), Universiti Kebangsaan Malaysia, 43600 UKM Bangi, Selangor, Malaysia
[c] Faculty of Industrial Sciences & Technology, Universiti Malaysia Pahang (UMP), Lebuhraya Tun Razak, 26300, Gambang, Kuantan, Pahang, Malaysia

ARTICLE INFO

ABSTRACT

An electrochemical Hg(II) ion sensor has been developed by using a miniaturized carbon paste screen-printed electrode (CSPE) modified with reduced graphene oxide (rGO) sheets and tris-thiourea (TTU) chelating ligand compound, i.e. N,N′,N″-((nitrilotris(ethane-2,1diyl))tris(azanediyl))tris(carbonothioyl))tribenz amide. In view of the strong cation-exchange characteristic and adsorption of aromatic TTU tridentate ligand on the graphene nanomaterial surface by non-covalent π–π stacking interaction, the differential pulse voltammetry (DPV) peak current response of the voltammetric sensor was linearly dependent on a broad Hg(II) ion concentration detection range from 0.1–00.0 mg L^{-1} with a limit of detection (LOD) estimated at 0.02 mg L^{-1} after accumulation for 10 min. The chemically modified miniaturized SPE showed high stability throughout the course of the sensor lifetime study for the detection of inorganic Hg(II) ion with a relative standard deviation (RSD) of the sensor response obtained at 1.2%. The electrochemical sensor is reusable up to three consecutive Hg(II) ion assays by using 0.05 M acetate buffer (pH 8) as the sensor regeneration solution with a reversibility RSD value of 3.9%. The voltammetric sensor based on TTU derivative element and rGO nanosheets revealed satisfactory selectivity for Hg(II) ion over a large number of potential interfering ions, e.g. Ca(II), Co(II), Cu(II), Fe(II), Ni(II), Na(I) and Zn(II), and demonstrated reliable quantitative results as compared to the results obtained with inductively coupled plasma-mass spectrometer (ICP-MS) standard method for Hg(II) ion detection in river water samples.

1. Introduction

Mercury is a naturally occurring metal exists mainly in three forms i.e. metallic element, inorganic salt and organic compound [1]. Since the 1930s, mercury has been widely used as a preservative in a number of biological and pharmaceutical products, including many vaccines, nasal spray, drop points, antiseptic and ointment diaper rashes [2]. Mercury is very toxic and extremely bioaccumulative. Its presence in the water resources, such as river, ocean and lake where it is taken up by microorganisms can be concentrated in the fish or shellfish bodies in the form of methylmercury [CH$_3$Hg(I)], and undergoing biomagnification to eventually confer toxicity in aquatic lives [3,4]. Consumption of contaminated seafoods and fish products is the major route of human exposure to mercury toxicity [5]. In the cement industry, mercury exposure among the workers could result in chronic asthma and bronchitis heart attacks. As such, the emission of mercury either by natural resources or anthropogenic activities can have a wide range of negative impacts on humans, plants and wild lands [6].

Conventional methods for detection of inorganic mercury and organic mercury compounds [e.g. ethylmercury [C$_2$H$_5$Hg(I) and CH$_3$Hg(I)] in the blood and seafood samples have been using liquid chromatography-inductively coupled plasma-tandem mass spectrometry (LC-ICP-MS) with a rapid ultrasound-assisted extraction procedure [7,8]. Combination of diffusive gradient in a thin film probe and ion chromatography coupled to ICP-MS (IC-ICP-MS) has been deployed by Hong et al. [9] for in situ simultaneous quantification of CH$_3$Hg(I) and mercury(II) [Hg(II)] ion in aquatic environments. By integrating a chip-based magnetic solid-phase microextraction system with micro high-performance liquid chromatography (microHPLC)–ICPMS, it can be used for speciation analysis of mercury [Hg(I) or CH$_3$Hg(I)] in HepG2 cells to understand its cytotoxicity effect and cell protection mechanism [10]. Detection of Hg(II) ion concentration in water and wastewater can be done by using cold vapor atomic absorption spectrometry (CV-AAS) [11]. However, a major problem with coupled chromatographic and atomic spectroscopic procedures is achieving the necessary detection limits for target analyte either in waters or volatile forms,

* Corresponding author.
 E-mail addresses: aishah80@ukm.edu.my, (S.A. Hasbullah), ckfeng@ump.edu.my, (K.F. Chong), lingling@ukm.edu.my. (L.L. Tan).

whereby preconcentration of the targeted species followed by coupling of effective derivatization is normally necessary prior to the detection step. Although laboratory techniques are routinely used for the analysis of metal ions as they are generally characterized as having high reliability, however laboratory-based methods very often are costly, require skills to execute and not to mention that they are time consuming. Thus, simple and portable device for rapid analysis of heavy metal contaminants, which is complementary to the traditional laboratory techniques is greatly demanded.

For this reason, the development of sensing devices e.g. chemical sensor or biosensor that will allow rapid and on-site analysis of inorganic mercury has gained increasing interest among researchers. Potentiometric sensor has been exploited for the determination of Hg(II) ion using tert-butylcalix[4]arene-tetrakis(*N,N*-dimethylthioacetamide) as anion-selective ionophore and tridodecylmethylammonium chloride as ion exchanger. An asymmetric membrane rotating ion-selective electrode configuration is required to improve the detection sensitivity, and dilution of the water sample is needed to allow practical application of the potentiometric sensor [12]). The Hg(II) ion sensor based on anodic stripping voltammetry (ASV) utilizing carbon nanoparticles-modified screen-printed electrode (SPE) is described by Aragay et al. [13]. However, heating treatment at 40 °C is necessary to increase the edge-like planes of the modified electrode for greater surface area available for metals deposition and electron transfer enhancement, thereby an enhanced electroanalytical performance over detection of Hg(II) can be achieved. A disposable bismuth SPE modified with multi-walled carbon nanotubes (MWCNTs) was developed by Niu et al. [14] for electrochemical stripping measurement of Hg(II) concentration with square-wave anodic stripping voltammetry (SWASV). In order to minimize the cost in mass production of modified electrodes considering a large number of samples is required for generating a high-quality analysis result. Therefore, a cost-effective alternative to the disposable type of sensing electrode would be a more economical substitution for it.

Among analytical methods, electrochemical methods have been shown to have more advantages compared to other analytical methods due to their portability, low cost, good selectivity and high sensitivity for electroanalytical determination of different types of compounds, such as drugs, food and environmental pollutants [15]. With this, a wide-ranging effort has been made to modify the electrode surface with various conductive nanomaterials in order to increase the electron transfer rate for significant enhancement of the resulting electrode sensitivity, which is the reason why surface modification with nanomaterials is important to sensor/biosensor performance. A novel analytical strategy for the detection of *N*-hydroxysuccinimide water pollutant was achieved by carbon paste electrode (CPE) amplified with tri-component nanohybrid composite of platinum nanoparticle/polyoxometalate/two-dimensional hexagonal boron nitride nanosheets and 1-hexyl-3-methylimidazolium chloride as conductive mediators [16]. The application of palladium-nickel nanoparticles decorated on functionalized-MWCNT was employed as a sensitive non-enzymatic electrochemical glucose sensor [17]. A highly sensitive electrocatalytic sensor was fabricated with a new nickel-based co-crystal complex electrocatalyst incorporated with NiO dope Pt nanostructure hybrid as conductive mediator on the CPE matrix for the determination of cysteamine and serotonin in the drug and pharmaceutical serum samples [18]. Simple modification of CPE electrode with novel modifiers composed of MWCNTs and a series of noncyclic crown-type polyether ligands along with a room temperature ionic liquid was employed for measuring thallium(I) in some natural waters without interference from sample matrix using differential pulse anodic stripping voltammetry (DPASV) method [19]. The hybrid nanocomposite of MWCNTs and magnetic nanoparticles functionalized with tannic acid and Au nanoparticles deposited on the glassy carbon electrode (GCE) showed excellent electrochemical oxidation of 17α–ethinylestradiol with electrochemical current increased by 28 times compared to the conventional GCE [20]. Thiophene and *p*-phenylenediamine were utilized as monomers to prepare low band gap copolymer and nanocomposites with core–shell construction by a simple in situ emulsion polymerization. The electrical conductivity of the nanocomposites is considerably higher than the copolymer which is dependent on the iron

content and doping degree [21]. A non-enzymatic amperometric hydrogen peroxide (H_2O_2) sensor was fabricated by incorporating novel nanostructured orthorhombic vanadium pentoxide into the CPE electrode, which provides significant catalytic activities for H_2O_2 reduction [22]. Electrochemical aptasensor using gold nanoparticles (AuNPs) immobilized on functional cupper magnetic nanoparticles and MWCNTs modified with aptamer and 6-mercapto-1-hexanol [23], or immobilized on a conjugate between MWCNT and thiol-functionalized magnetic nanoparticles [24] that were modified with an aptamer showed ultra-sensitivity towards label free detection of bisphenol A (BPA) due to a synergistic augmentation on the surface of the modified electrode. Direct electro-oxidation of BPA was later achieved by utilizing novel nanocomposite based on MWCNT/thiol functionalized magnetic nanoparticles as an immobilization platform and AuNPs as an amplifying electrochemical signal [25].

Reduced graphene oxide (rGO) or known as graphene material possesses superior mechanical, electrical and thermal properties by virtue of the highly mobile π electrons that are located above and below the graphene sheet [26]. It is an effective adsorbent towards any chemical or biological compound having aromatic rings to strongly adsorb at the graphene or graphene oxide surface [27]. A composite film consisted of polyacrylate and rGO nanosheets casted on the SPE with immobilized hemoglobin protein has been reported in the electrocatalytic reduction of nitrite study by Raja Jamaluddin et al. [28]. In addition, graphene oxide sheets can be an ideal substrate for the study of enzyme immobilization as they are enriched with oxygen-containing groups, which makes them possible to immobilize enzymes without any surface modification or any coupling reagents [29]. A CPE electrode modified with copper oxide decorated rGO, with 1-methyl-3-octylimidazolium tetrafluoroborate as a binder has been developed for high performance simultaneous determination of cholesterol, ascorbic acid and uric acid [30]. An electrochemical As(III) ion sensor fabricated by casting graphene oxide/zinc based metal-organic nanocomposite on a GCE electrode, followed by an electrochemically reduction of graphene oxide was performed by DPASV showed excellent electrochemical performance, such as a wide linear range at part per billion levels [31]. And, there are a lot more reports demonstrating the adaptation of graphene nanomaterials for the applications of DNA detection either as a label-free or amplification-free approach [32].

Thiourea derivative compound i.e. selenolthiol has been shown capable of capturing Hg(II) ion on mammalian by demonstrating enhanced inhibition activity as a result of detoxification mechanism of NADPH-reduced thioredoxin reductase (TrxR) as an implication for treatment of mercury poisoning [33]. A thiourea-based chemosensor was developed by Vonlanthen et al. [34] to be employed for fluorescence microscopy imaging of Hg(II) ion concentration in living mammalian cells. Additionally, modification of label-free gold nanoparticle (AuNP) as a probe for colorimetric Fe(II) ion detection has been reported to occur in acidic thiourea mixture as medium to catalyze the leaching of gold at room temperature [35].

In this study, we demonstrate the application of reduced graphene oxide (rGO) as both superb conducting platform for efficient electron transfer and immobilization platform for binding with tris-thiourea (TTU) chelating agent on the miniaturized carbon paste screen-printed electrode (CSPE). In view of the TTU aromatic species, which is rich in π orbitals, it can be strongly adsorbed onto aromatic macromolecules such as graphene materials through π-π staking interaction. Preliminary study by means of UV–Vis spectrometry titration revealed the TTU-Hg(II) complex with tridentate coordinated ligand systems, whereby the presence of thioamide (NHCS) and (NHCO) amide groups in TTU ionophore were acted as specific binding sites for binding with Hg(II) ions via coordinate covalent bonds. The conditions used for electrochemical differential pulse voltammetric (DPV) determination of Hg(II) concentration e.g. pH, accumulation time, dynamic linear range, reversibility, selectivity and long term stability were optimized. The applicability of the TTU-rGO-modified CSPE for the determination of inorganic Hg(II) ion has been assessed in river water by a simple filtration. The schematic diagram showing the stepwise fabrication of electrochemical Hg(II) sensor based on CSPE electrode modified with graphene nanosheets and TTU organic ligand, and the multiple binding sites for reaction with Hg(II) ions is displayed in Fig. 1.
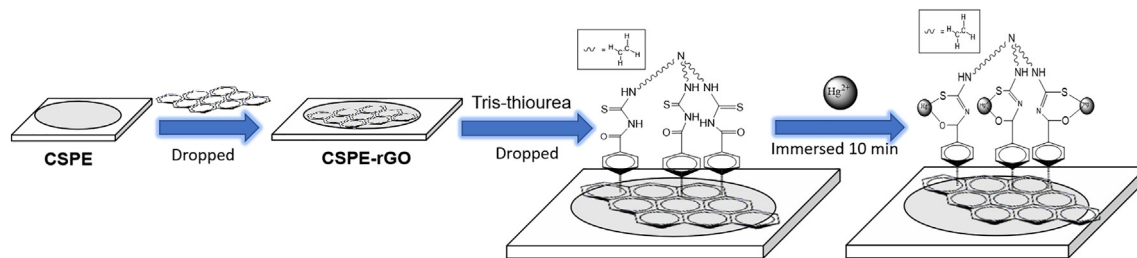
Fig. 1. Schematic diagram of the steps of the fabrication process for electrochemical Hg(II) sensor based on CSPE electrode modified with rGO nanosheets immobilization matrix and TTU polydentate ligand chemical sensing reagent as well as the active sites involved in binding with Hg(II) ion.

2. Experimental

2.1. Instrumentation

The Fourier transform infrared (FTIR) spectrum of the tris-thiourea (TTU) ligand derivative was recorded in the wavenumber range of 4000–400 cm^{-1} by using Perkin Elmer Spectrum GX spectrophotometer. ^{1}H and ^{13}C nuclear magnetic resonance (NMR) experiments were performed on a Bruker Advance III 400 MHz instrument utilizing DMSO-$_{d6}$ as a solvent. Single-crystal X-ray diffraction (SXRD) investigations were performed on a Bruker D-QUEST diffractometer with graphite monochromated Mo and Cu-K$_\alpha$ radiation (0.71073 and 1.54178 Å). Preparation of homogenous mixture containing reduced-graphene oxide (rGO) and TTU ligand compound was conducted by using Elmasonic sonicator. The measurement of pH for 0.05 M acetate buffer was made with Metrohm pH meter. Field Emission Scanning Electron Microscopy (FESEM) was used to study the surface morphology and size distribution of rGO and immobilized TTU compound on the rGO-modified carbon paste screen printed electrode (CSPE). Differential pulse voltammetry (DPV) and cyclic voltammetry (CV) were conducted using Autolab PGSTST electrochemical workstation (Netherlands). The three-electrode setup consists of a CSPE modified with rGO and TTU derivative element as the working electrode, a platinum counter electrode and a Ag/AgCl reference electrode. Inductively coupled plasma-mass spectrometer (ICP-MS) was employed to validate the electrochemical Hg(II) ion in river water matrices.

2.2. Reagents and solutions

All the chemicals and reagents used in this study were of analytical grade and were used as received without any further purification. All solutions were prepared with deionized water of resistivity not less than 18.2 MΩ cm^{-1}. Graphite powder, sulfuric acid (H$_2$SO$_4$, 95–98%), potassium persulfate (K$_2$S$_2$O$_8$, 98%), phosphorus pentoxide (P$_2$O$_5$, 99%), potassium permanganate (KMnO$_4$, ≥99%), potassium hydroxide (KOH, ≥85%) and hydrazine monohydrate (NH$_2$NH$_2$·H$_2$O, 98%) were supplied by Sigma-Aldrich and were utilized in the synthesis of reduced graphene oxide (rGO). Benzoyl chloride (C$_6$H$_5$COCl, 99%), ammonium thiocyanate (NH$_4$SCN, ≥97.5%) and tris(2-ethylamino) ethanol (C$_8$H$_{21}$N$_3$O, ≥98%) were obtained from Aldrich and were used in the synthesis of TTU chelating compound. 0.05 M acetate buffer from pH 3 to pH 8 was prepared by mixing appropriate amount of 0.05 M glacial acetic acid (CH$_3$COOH, R & M Chemicals, 100%) with 0.05 M sodium acetate (CH$_3$COONa, Friendemann Sdhmidf Chemical, 99%). Mercury(II) acetate [Hg(CH$_3$COO)$_2$, ACS Reagent, ≥98%] was prepared in 0.05 M acetate buffer (pH 3). 0.01 M potassium ferricyanide (K$_3$[Fe(CN)$_6$], ACS Reagent, >99%) was prepared by dissolving 0.165 g K$_3$[Fe(CN)$_6$] in 50 mL of 0.05 M acetate buffer at pH 3.

2.3. Synthesis of rGO

rGO was synthesized according to the methods which have been described elsewhere [28]. In general, GO was prepared by using natural graphite powder through a modified Hummers and Offeman method [36]. Prior to the synthesis of GO procedure, a graphite oxidation procedure

was first carried out according to the protocol recommended by Kovtyukhova et al. [37] in order to avert the formation of graphite-core/GO-shell particles in the final product as a result of incomplete oxidization reaction. The precursor of GO was then dispersed in deionized water followed by the addition of KOH solution as a strong base so as to afford a large negative charge through reactions with hydroxyl, epoxy and carboxylic acid functional groups on the GO sheets and that yielded an extensive coating of the sheets with negative charges and K$^+$ ions [38]. 0.25 mL of 100 mmol hydrazine monohydrate was added to the KOH-treated GO to produce a homogeneous yellow-brown aqueous suspension GO. The as-obtained GO suspension was ultrasonicated and heated in an oil bath at 95 °C for 24 h to gradually produced the rGO as a black solid precipitate. The as-synthesized rGO was eventually washed with abundant deionized water followed by acetone, and dried in a vacuum desiccator.

2.4. Synthesis of TTU organic ligand

TTU chelating ligand was synthesized according to the method described by Misral et al. [39] with slight modifications. As Fig. 2 signifies, the TTU ionophore compound was prepared by mixing 1 mmol of benzoyl chloride (**a**) with 1 mmol of ammonium thiocyanate (**b**) in acetone under stirring for 15 min at 60 °C. The white precipitate of NH$_4$Cl (**d**) was filtered, and the yellowish solution of benzoyl isothiocyanate intermediate (**c**) was directly reacted with 0.3 mmol of tris(2-ethytlamino) ethanol (**e**) in an ice bath under continuous stirring for about 5–6 h. The white TTU precipitate formed was washed several times with deionized water and dried in a vacuum desiccator.

2.5. Fabrication of electrochemical Hg(II) ion-selective sensor

The electrochemical Hg(II) ion sensor based on CSPE modified with rGO and TTU was prepared by first dispersing 1 mg of rGO in 200 μL of ethanol to form a stabilized colloidal rGO sheets suspension. Homogenous TTU solution with concentration of 15 mM, on the other hand, was prepared by dissolving 0.0653 g of TTU compound in 200 μL of ethanol followed by ultrasonication for 30 min. The CSPEs used were designed by Universiti Kebangsaan Malaysia and manufactured by Scrint Technology Pvt. Ltd., Malaysia with an electrode diameter of 4 mm and an active surface area estimated at 12.57 mm^2. The CSPE was drop-coated with 15 μL or colloidal rGO sheets and left to dry at room temperature (25 °C) before dispensing 15 μL of TTU solution on the rGO electrode, and dried at ambient conditions. The electrochemical conductivity of the TTU-grafted rGO (TTU-rGO) electrode and its response with Hg(II) ion was measured by CV and DPV techniques versus Ag/AgCl reference electrode, and 10 mM K$_3$[Fe(CN)$_6$] electroactive probe in 0.05 M acetate buffer at pH 3 was used as supporting electrolyte.

2.6. Optimization of voltammetric Hg(II) ion-selective sensor

Optimization of electroanalytical performance of the TTU derivative-based Hg(II) ion sensor was conducted by means of DPV and K$_3$[Fe(CN)]$_6$ was used as the redox probe. pH effect on the Hg(II) ion sensor was investigated by immersing six individual TTU-rGO electrodes into the respective
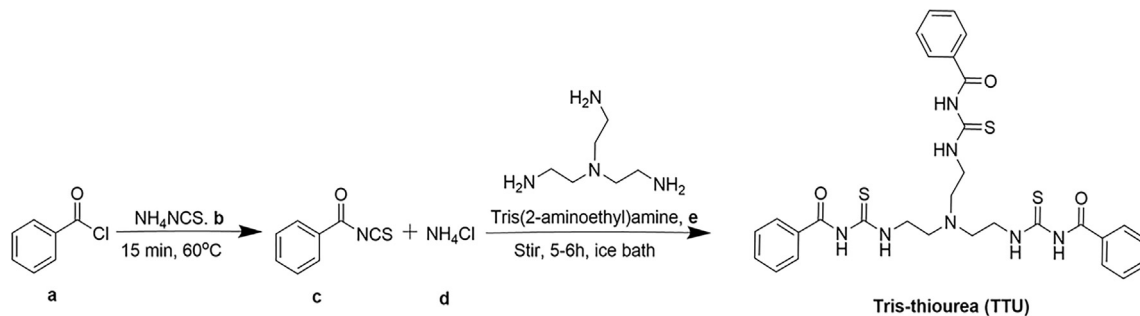
Fig. 2. The chemical reactions involved in the synthesis of TTU chelating ligand.

100.0 mg L^{-1} Hg(II) ion solutions at pH 3, pH 4, pH 5, pH 6, pH 7 and pH 8 (0.05 M acetate buffer) for 10 min before DPV peak current response was measured. Accumulation time of the sensor was performed by dipping the TTU-rGO electrode into 90 mg L^{-1} Hg(II) ion in 0.05 M acetate buffer at pH 3 for 1 min, 2 min, 5 min, 7 min, 10 min and 15 min before electrochemical response was recorded at DPV anodic peak current of 0.23 V. The electrochemical DPV response of the TTU-rGO based sensor towards determination of different levels of Hg(II) ion concentrations was carried out by using 0.1 mg L^{-1} to 180.0 mg L^{-1} Hg(II) ion in 0.05 M acetate buffer at pH 3. The life span of the electrochemical Hg(II) ion sensor was determined by measuring the voltammetric response of three chemically modified electrodes with 20.0 mg L^{-1} Hg(II) ion. The DPV measurement of the sensor was performed periodically within 38 days. The regeneration study was conducted by using 0.05 M acetate buffer (pH 8) as a regenerating agent. The TTU-rGO modified CSPE was immersed in 0.05 M acetate buffer at pH 8 for 10 min for removal of the Hg(II) ion after every Hg(II) ion measurement at 80 mg L^{-1} was done using the modified electrode. The selectivity study for Hg(II) ion sensor was tested using Ca(II), Co(II), Cu(II), Fe(II), Ni(II), Na(I) and Zn(I) ions during determination of 80 mg L^{-1} Hg(II) ion at different molar ratios between Hg(II) ion and interfering ion i.e. 1.0:0.1, 1.0:1.0 and 1.0:10.0. All the electroanalytical experiments were performed in triplicate.

2.7. Voltammetric Hg(II) ion chemical sensor for real sample analysis

This study performed by using river water samples collected from two different points along Langat River, Selangor, Malaysia. Two sterilized polyethylene bottles were used for water sampling. The river water was filtered using Whatman filter paper No.1 to remove suspended particles. The river water pH was then adjusted to pH 3 by adding 0.05 M glacial acetic acid and 0.05 M sodium acetate. 80 mg L^{-1} and 100 mg L^{-1} Hg(II) ions were spiked into the river water sample, and examined by using the developed Hg(II) ion electrochemical sensor and validified with ICP-MS standard method.

3. Results and discussion

3.1. Characterization of TTU ligand compound and immobilization on the rGO nanomaterial

The as-prepared TTU organic ligand was obtained as white solid powder (yield: 2.07 g, 89%) with melting point of 257–269 °C. Chemical characterization of the TTU compound was conducted by using spectroscopy methods e.g. FTIR, ^{1}H NMR, ^{13}C NMR and single crystal X-ray diffraction analysis. The FTIR spectrum of the thiourea derivative (Fig. S1) shows strong absorption band at 3186 cm^{-1}, which confirms the presence of NH functional group. The two most distinctive FTIR bands at 1660 cm^{-1} and 1527 cm^{-1} are associated with the carbonyl (CO) and thiono (CS) functional groups of the TTU ligand compound. ^{1}H NMR analysis of TTU derivative showed characteristic peaks at δ 10.93 ppm and δ 8.94 ppm, which indicate the presence of thioamide (NHCS) and (NHCO) amide group (Fig. S2). This is also strongly supported by ^{13}C NMR measurements

(Fig. S3) that indicates chemical shift at δ 207.07 ppm and δ 179.93 ppm, which confirms the presence of CS and CO groups. The downfield chemical shifts of functional groups in ^{1}H and ^{13}C NMR are due to anisotropic and electronegative effect of oxygen and sulfur atom [40]. SXRD investigation revealed that the TTU ligand is in the crystalline form as two non-centrosymmetric molecules in one-unit cell (Fig. S4) having triclinic system with space group of *P*1. The crystallographic data of the as-synthesized TTU ligand derivative is tabulated in Table S1.

Chemical and physical characterization of rGO have been described in previous paper [28]. Fig. 3a shows the field emission scanning electron micrograph of the as-synthesized rGO that is ultrathin, flexible, sheet-like and transparent wrinkled-type [41] with average thickness of 2–4 nm. As TTU organic ligand is introduced on the rGO surface, the loosely stacked morphology of TTU chemical receptor-functionalized rGO sheets (Fig. 3b) is anticipated to enhance the Hg(II) ion diffusion and migration rate, and that the electron transfer rate at the TTU-rGO electrode surface can thus be enhanced [42]. The TTU is grafted on the rGO sheets by π-π interaction or non-covalent bond through molecular stacking between aromatic carbon in graphene and aromatic group in TTU ligand [43,44].

3.2. Chemical interaction between TTU ligand and Hg(II) ion

The chemical reaction between TTU chelating ligand and Hg(II) ion has been performed in un-immobilized state using DMSO as the solvent at three different molar concentration ratios of 1:1, 1:2 and 1:3 between TTU and Hg(II) ion. The colourless mixed TTU/Hg(II) ion solution dramatically turned into light yellow solution as increasing the molar concentration of Hg(II) ion from 0.001–0.003 M, whilst TTU concentration remained constant at 0.001 M of the mixed solutions (Fig. S5). This was attributed to the ionochromic behavior of the TTU ligand towards Hg(II) ion, i.e. mercury ionophore [45].

In addition, UV–Vis spectroscopy titration was also carried out to determine stoichiometry ratio of TTU-Hg(II) chelate complex by gradual addition of 150 μL of 0.01 M Hg(II) ion into 0.001 M TTU ligand until a slight sigmoidal curve is observed on the spectroscopic titration curve (inset of Fig. S6), which indicates a conformational change to the ligand is occurred. By drawing and extrapolating the standard lines in the molar-ratio curve, the TTU-Hg(II) complex establishes stoichiometry ratio of 1:3, which implies one TTU molecule binding to three Hg(II) ions via a lone pair on the respective oxygen and sulfur atoms of the TTU derivative donating to the Hg(II) ion through coordinate covalent bonds. A bathochromic shift of the absorption peak from 230 nm to 235 nm is observed along with the hyperchromic shift (Fig. S6) upon UV–Vis spectroscopy titration of TTU tridentate ligand with Hg(II) ion suggests the conceivable formation of host-guest chelate of TTU-Hg(II) [46].

3.3. Electrochemical characterization of TTU-rGO modified CSPE electrode

Fig. 4 represents the cyclic voltammograms of bare CSPE electrode and modified CSPE with rGO and TTU ionophore as well as before and after the electrochemical sensor reacted with 10.0 mg L^{-1} Hg(II) ion at pH 3 in the presence of 10 mM K$_3$[Fe(CN)$_6$], which functioned as the electroactive
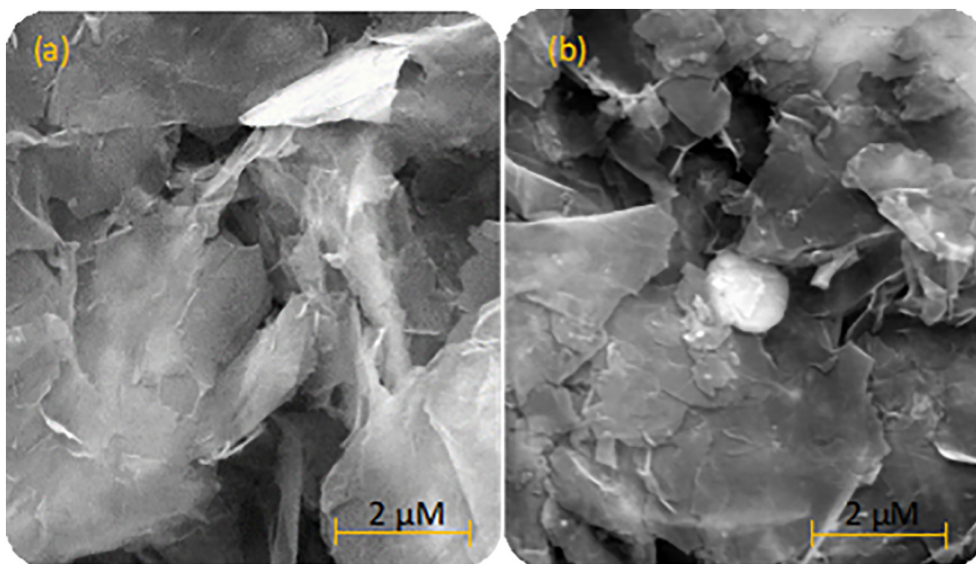
Fig. 3. FESEM images of (a) rGO sheets and (b) TTU-modified rGO materials at $25000\times$ magnification.

mediator. The bare CSPE demonstrated rather lacking electronic conductivity (blue line) and that modification of the CSPE with graphene material is necessary to improve the electrochemical response of the electrode. The presence of the rGO nanosheets on the CSPE had shown to improve the heterogeneous electron transfer of the electrode [47] with both well-defined anodic peak current (I_{pa}) and cathodic peak current (I_{pc}) of $K_3[Fe(CN)_6]$ redox indicator are discernible at 0.40 V and 0.08 V, respectively (red line). Further modification of the rGO electrode with TTU tridentate chelating ligand via non-covalent π-π staking between benzene rings of TTU ionophore and hexagonal cells of graphene sheets depicted higher voltammetric response (green line). This was ascribed to the immobilized rGO sheets, which has increased the electrochemical active area on the CSPE and provided stable mobility of electron [27]. After preconcentration of the TTU-rGO electrode in Hg(II) ion solution for 10 min, a remarkable increment in the electrochemical response was noticeable (purple line). This was due to the fact that the TTU multidentate ligand, which consisted of electron donor groups (Lewis base) bonded to the electron acceptor, i.e. the metal ion (Lewis acid), and when the electron from the donor transf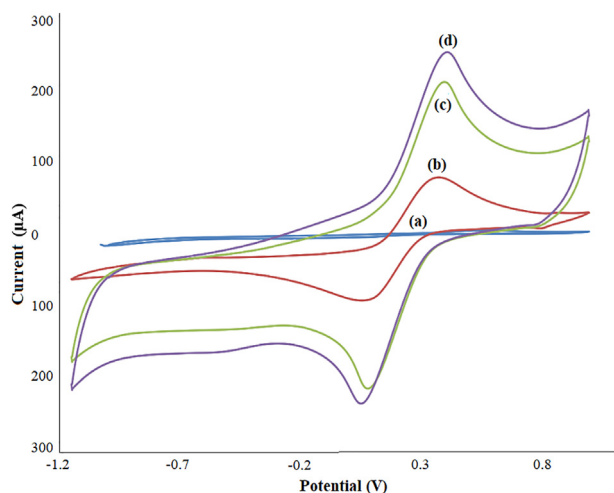erred to the orbital d of the electron acceptor group, it produced a kind of internal oxidation/reduction process due to changes in oxidation states [48]. The electrochemical detection of Hg(II) ion using this chemically modified rGO electrode can thus be transduced into electrical signal based on the reversible redox reaction of the $K_3[Fe(CN)_6]$ electron shuttling agent.

3.4. Electroanalytical performance of TTU ionophore-based Hg(II) ion sensor

The DPV peak current response of the Hg(II) ion chemical sensor as a function of pH is illustrated in Fig. S7 in the supplementary material. The electrochemical response of the Hg(II) ion sensor was noticed to decline steadily with increasing pH value of 0.05 M acetate buffer from pH 3 to pH 8, therefore the optimum pH for metal-chelation reaction was remained constant at pH 3 in the next electroanalytical optimization experiments. In acidic condition, i.e. pH 3, the optimum reaction medium can contribute to tautomeric effect of the immobilized TTU chelating ligand, and promoted deprotonation reaction of thioamide group to form complex assembly with Hg(II) ion as presented in Fig. S8 in the supplementary material [49]. At higher pH conditions, i.e. greater than pH 3 and towards alkaline medium, H^+ ions were depleted and Hg(II) ions were prone to exchange with exchangeable OH^- ion to form mercury(II) hydroxide $[Hg(OH)_2]$ as a result of ion exchange reaction [50]. In view of the metal-chelation reaction is pH-dependent, high pH would result in both thioamide and amide functional groups of TTU ligand *no* longer efficient to participate in metal binding at all.

The time dependent DP*V* response of the Hg(II) ion sensor showed gradual increase in the electrochemical voltammetric response from 1 min to 10 min pre-concentration time of TTU-rGO electrode in Hg(II) ion solution (Fig. S9). As the highest sensor response was obtained at 10 min of accumulation of the sensor electrode in Hg(II) ion solution at pH 3. This signifies maximum chelation reaction has attained at the electrode surface. However, after prolonged incubation of the electrochemical sensor in analyte solution above 10 min, it has reduced the efficiency of $K_3[Fe(CN)_6]$ redox mediator transferring electron to the electrode surface and that a slight decrease in the sensor response was perceived.

The voltammetric pattern of the Hg(II) ion sensor is characterized by DP*V* I_{pa} at 0.23 V. The DPV response of the TTU polydentate ligand-based sensor over electrochemical quantification of Hg(II) ion in the concentration range of 0.1 mg L^{-1} to 180.0 mg L^{-1} at 0.23 V and pH 3 is shown in Fig. 5a. The corresponding differential pulse voltammograms of the Hg(II) ion sensor response is exhibited in the inset of Fig. 5a. The electrochemical sensor response increased proportionally with increasing the Hg(II) ion

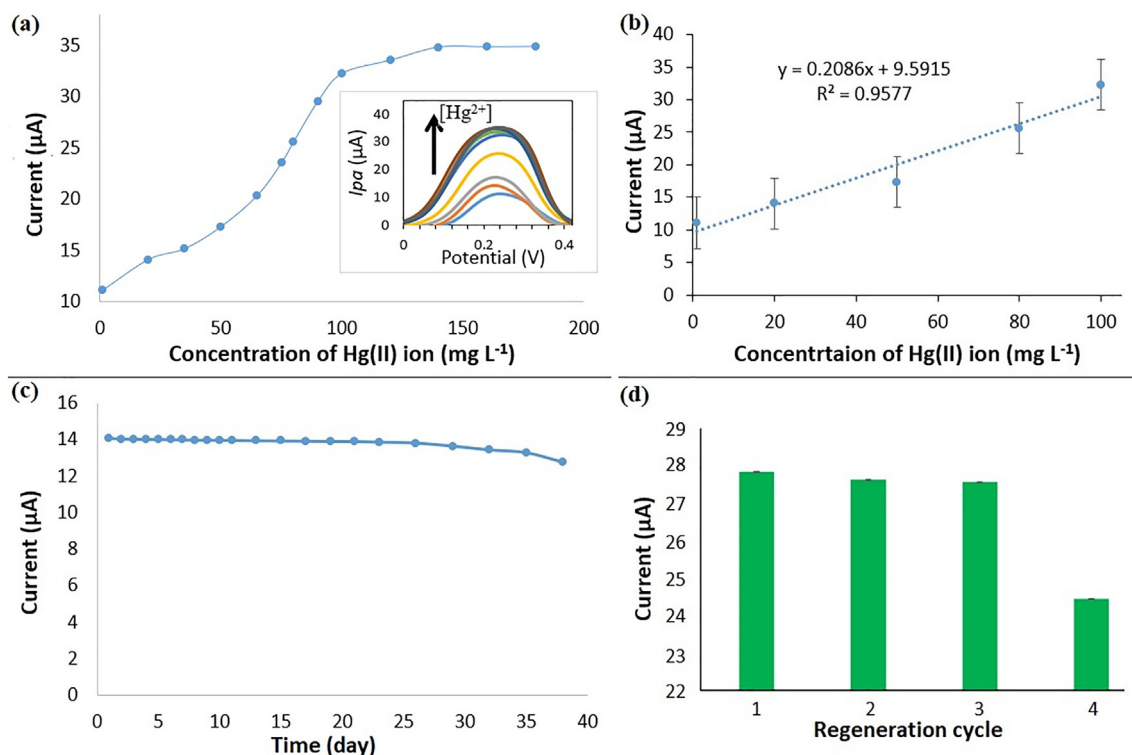**Fig. 4.** Cyclic voltammograms of (a) Bare CSPE (blue line), (b) rGO CSPE electrode (red line), (c) TTU-rGO modified CSPE (green line) and (d) Hg(II)-TTU-rGO modified CSPE (purple line) in 0.05 M acetate buffer (pH 3) containing 10 mM $K_3[Fe(CN)_6]$.

Fig. 5. (a) The electrochemical sensor response with different Hg(II) ion concentrations between 0.1 mg L^{-1} and 180.0 mg L^{-1} in 0.05 M acetate buffer (pH 3) 0.23 *V*. The inset shows the corresponding differential pulse voltammograms of the Hg(II) ion chemosensor. (b) The calibration curve of the optimized TTU-rGO based Hg(II) ion electrochemical sensor from 0.1 mg L^{-1}-100.0 mg L^{-1}. (c) The shelf life trending of the volltammetric Hg(II) ion sensor for an experimental period of 38 days towards determination of 20.0 mg L^{-1} Hg(II) ion. (d) The DPV peak current response of the Hg(II) ion sensor for four consecutive measurements of 80 mg L^{-1} Hg(II) ion and regeneration of the sensor electrode using 0.05 M acetate buffer at pH 8.

concentration from 0.1–100.0 mg L^{-1} as metal-chelation reaction rate increased as increasing the analyte concentration. This allowed higher diffusion rate of K$_3$[Fe(CN)$_6$] redox probe to accelerate the redox reaction, and to facilitate the mediated electron transfer reaction at the electrode-electrolyte interface. The sensor response become saturated thereafter due to thioamide and amide functional groups of TTU chemical sensing phase were occupied by Hg(II) ion via dative covalent bonds. nd reproducibility relative standard deviation (RSD) of the sensor response was calculated at 4.9%. The limit of detection (LOD) of the voltammetric Hg (II) ion sensor calculated using the equation LOD = 3 s/m, where 's' is the average standard deviation of blank and 'm' is the slope of the calibration curve [51] was estimated at 0.02 mg L^{-1} Hg(II) ion.

The lifetime performance of the TTU-rGO-modified CSPE electrode is illustrated in Fig. 5c. The electrochemical sensor was found to be tremendously stable throughout the course of the experiment towards determination of 20.0 mg L^{-1} Hg(II) ion, and the DPV peak current response of the sensor decreased slightly or not more than 95% of its initial

response after 35 days of storage period. This was largely due to the strong adsorption of aromatic TTU sensing ionophore on the basal plane of the immobilized rGO nanosheets by π–π stacking on the CSPE, and thus preserving the electronic conductivity of graphene materials from physical or chemical structure interference. The electrochemical sensor showed high stability in the detection of inorganic Hg(II) ion right through the experimetal period of 35 days with a RSD acquired at 1.2%.

Sensor repeatability was evaluated via four consecutive binding and regeneration cycles of the TTU-rGO electrode. As Fig. 5d indicates, 100% of the sensor response was remained after three consecutive binding and regeneration cycles of the sensor electrode. The use of 0.05 M acetate buffer at pH 8 as the regeneration solution has literally reacted with immobilized TTU-Hg(II) chelate complex by removing the bound Hg(II) ion from the TTU-rGO electrode, and Hg(OH)$_2$ was precipitated out to regenerate the sensor electrode for next metal-chelation reaction by using 80 mg L^{-1} Hg (II) ion. The repeatability RSD of the sensor was calculated at 3.9%. However, when the TTU-rGO-based sensor was undergoing the fourth binding and regeneration cycle, the electrochemical sensor response dropped to

Table 1

The percentage interference effect of various interfering ions e.g. Ca(II), Co(II), Cu(II), Fe(III), Ni(II), Na(I) and Zn(II) ions on the electrochemical Hg(II) ion sensor response at Hg(II):interfering ion molar ratios of 1.0:0.1, 1.0:1.0 and 1.0:10.0.

Interfering ion	Interference level (%)			
	Molar ratio of Hg(II):interfering ion			
	1.0:0.0	1.0:0.1	1.0:1.0	1.0:10.0
Ca(II)	0	18.53 ± 0.05	22.06 ± 0.04	30.65 ± 0.00
Co(II)	0	0.97 ± 0.02	5.68 ± 0.04	8.61 ± 0.03
Cu(II)	0	27.78 ± 0.09	42.27 ± 0.007	43.41 ± 0.05
Fe(III)	0	4.65 ± 0.05	17.14 ± 0.06	17.70 ± 0.07
Ni(II)	0	3.29 ± 0.06	3.97 ± 0.08	8.60 ± 0.06
Na(I)	0	22.00 ± 0.08	24.30 ± 0.04	26.13 ± 0.08
Zn(II)	0	24.01 ± 0.03	28.49 ± 0.09	34.72 ± 0.09

Table 2

Validation of the electrochemical sensor based on TTU-rGO modified CSPE electrode with ICP-MS standard method for quantification of Hg(II) ion concentration in river water matrices.

Method	Spiked Hg(II) ion concentration (mg L^{-1})	Sample A	Sample B
		Found Hg(II) ion concentration (mg L^{-1})	
TTU-rGO modified CSPE	80	76.01 ± 0.03	74.32 ± 0.08
	100	93.28 ± 0.07	97.87 ± 0.03
ICP-MS	80	79.34 ± 0.00	79.83 ± 0.00
	100	99.60 ± 0.00	98.29 ± 0.00

Table 3

Performance comparison study of developed Hg(II) ion chemical sensor with other reported electrochemical sensors for Hg(II) ion detection.

Materials/compound/electrode	Application mode	Accumulation time (min)	LOD (mg L^{-1})	Sensor lifetime (day)	Reference
Sodium montmorillonite/CSPE	disposable	9	1.0030×10^{-6}	–	Huang et al. [54]
Sumichelate Q10R/CSPE	disposable	10	1.2035×10^{-5}	–	Ugo et al. [55]
CBNP-AuNP nanocomposite/CSPE	disposable	7	0.0002	–	Cinti et al. [56]
Graphite nanoparticle/SPE	reusable	2	50.1475	30	Aragay et al. [13]
MWCNTs/bismuth SPE	disposable	3	0.9027	–	Niu et al. [14]
N220 CB film/SPE	disposable	–	0.0001	–	Arduini et al. [57]
TTU-rGO/CSPE	reusable	10	0.0261	35	This work

50% of its original response, which might be due to decomposition of the thiourea chemical receptor at the rGO electrode.

3.5. Selectivity of the Hg(II) ion electrochemical sensor

To establish specificity of the sensor in detecting Hg(II) ion, interference study was conducted against some metal ions e.g. Ca(II), Co(II), Cu(II), Fe(III), Ni(II), Na(I) and Zn(II) ions with the same electrochemical detection procedure implemented for Hg(II) ion. As shown in Table 1, among these potential interfering metal ions, Ca(II), Cu(II), Na(II) and Zn(II) ions presented more than ±5% interference effect to the electrochemical quantitation of 80 mg L^{-1} Hg(II) ion at Hg(II):interferent molar concentration ratio of 1.0:0.1. This is in accordance with the principle of Pearson soft and hard acid-base (HSAB), whereby the immobilized TTU sensing ligand acted as soft base and that having most intense interaction with mild to soft Pearson acidic ion that includes metal ions, such as Ca(II), Cu(II), Na(II) and Zn(II) ions driven by simple electron transfer effect, and rendered competitive binding of the foreign metals ion with target Hg(II) ion for binding sites at the TTU ligand [46]. Nevertheless, according to the National Water Quality Standards for Malaysia [52], these metal ions are not exist in livestock drinking except Hg(II) ion at 0.004 mg L^{-1} in class III water (i.e. polluted water). As such, the interference effect from those potential interfering ions can be neglected upon detection of Hg(II) with the developed electrochemical sensor based on TTU-rGO modified CSPE. Otherwise, ethylenediaminetetraacetic acid (EDTA), a widely applicable masking agent could be used to form complexes with great affinity for Cu(II) and Zn(II) ions in a simple binary mixture or a more complex mixture [53].

3.6. Application of the TTU derivative-based Hg(II) ion sensor for river water sample analysis

The accuracy of the proposed chemically modified sensor based on screen printed electrode for Hg(II) ion quantification has been validated with ICP-MS conventional method. The river water samples spiked with known amount of standard Hg(II) ion concentration at 80 mg L^{-1} and 100 mg L^{-1} were analysed by both methods. Based on the comparison results between conventional ICP-MS and electrochemical sensor tabulated in Table 2, both methods showed comparable results for Hg(II) ion determination in river water samples with a maximum total error of lesser than ±7% for Hg(II) ion concentration results obtained by voltammetric chemical sensor compared to ICP-MS. This indicates the Hg(II) ion electrochemical sensor based on TTU-rGO modified CSPE is in good agreement with the ICP-MS standard method for Hg(II) ion detection.

3.7. Performance comparison study between TTU-rGO-based sensor and other electrochemical sensors for inorganic Hg(II) ion detection

A performance comparison study on Hg(II) ion sensor developed in this study and previously reported Hg(II) ion electrochemical sensors based on different conducting materials and chemical chelating compound immobilized on the SPE electrode, such as sodium montmorillonite-modified CSPE [54], sumichelate Q10R chelating resin containing dithiocarbamate groups-modified CSPE [55], carbon black-gold nanoparticle (CBNP-AuNP) nanocomposite-modified CSPE [56], graphite nanoparticle-

modified SPE [13], multi-walled carbon nanotubes (MWCNTs)-modified bismuth SPE [14] and N220 nanostructured carbon black (CB) film-modified SPE [57] is outlined in Table 3. The developed Hg(II) ion chemical sensor demonstrated the potential for rapid, economical and convenient analysis of Hg(II) without the need of skilled personnel or burdensome equipment in the field. The polydentate TTU ionophore possesses multiple active sites that could increase the binding reaction rate with Hg(II) ion [58]. Direct grafting of TTU derivative onto the rGO electrode via π-π stacking interaction between aromatic rings could keep its intrinsic electronic properties remained intact in order to maintain the high electrochemical performance and led to faster electron transfer [26,59]. The TTU-rGO-modified CSPE can simply be regenerated in 0.05 M acetate buffer at pH 8, and be reused for screening of Hg(II) ion at room temperature.

4. Conclusions

The electrochemical Hg(II) ion sensor fabricated from miniaturized CSPE with electrode surface modified with rGO sheets and TTU chemical receptors by an easy drop casting procedure making this approach extendible to an automatable mass preparation of the modified CSPEs. The excellent electrical conductivity of the graphene material and good compatibility with aromatic thiourea compound rendered high electrochemical sensing performance of Hg(II) analysis with good stability of the sensor electrode. The polydentate TTU chemical sensing ionophore permitted multiple interaction with Hg(II) ion has widen the chemical sensor detection range to allow direct screening of inorganic mercury in water samples without additional dilution step is required, and holds wide application prospects in both environmental and industrial monitoring. The regenerable screen-printed voltammetric Hg(II) ion sensor is affordable and economical where it minimizing the environmental footprint of chemical materials as the electrode is reusable.

Author's comment

We wish for a fast peer review process for speedy journal publication.

Declaration of Competing Interest

The authors declare no conflict of interest.

Appendix A. Supplementary data

Supplementary data to this article can be found online at https://doi.org/10.1016/j.jelechem.2020.114670.

References

[1] P.Y. Liao, C.W. Liu, W.Y. Liu, Bioaccumulation of mercury and polychlorinated dibenzo-p-dioxins and dibenzofurans in salty water organisms, Environ. Monit. Assess. 188 (2016) 1–15, https://doi.org/10.1007/s10661-015-5019-z.

[2] J.P. Baker, Mercury, vaccines, and autism: one controversy, three histories, Am. J. Public Health 98 (2008) 244–253, https://doi.org/10.2105/AJPH.2007.113159.

[3] J. Cortes, J. Peralta, R. Diaz-Navarro, Acute respiratory syndrome following accidental inhalation of mercury vapor, Clin. Case Rep. 6 (2018) 1535–1537, https://doi.org/10.1002/ccr3.1656.

[4] Y. Liu, G. Liu, Z. Yuan, H. Liu, P.K.S. Lam, Presence of arsenic, mercury and vanadium in aquatic organisms of Laizhou Bay and their potential health risk, Mar. Pollut. Bull. 125 (2017) 334–340, https://doi.org/10.1016/j.marpolbul.2017.09.045.

[5] S. Das, Bioaccumulation of mercury by the panaeid prawns from Rushikulya estuary, east coast of India, Indian J. Fish. 47 (2000) 301–310 Corpus ID: 88459358.

[6] A. Riaz, A. Khan, M.T. Shah, I. Din, S. Khan, Determination of mercury in the wild plants with their soils along Indus, Gilgit and Hunza rivers, J Himal. Earth Sci. 50 (2017) 35–40.

[7] B.L. Batista, J.L. Rodrigues, S.S. De Souza, V.C. Oliveira Souza, F. Barbosa, Mercury speciation in seafood samples by LC-ICP-MS with a rapid ultrasound-assisted extraction procedure: application to the determination of mercury in Brazilian seafood samples, Food Chem. 126 (2011) 2000–2004, https://doi.org/10.1016/j.foodchem.2010.12.068.

[8] J.L. Rodrigues, S.S. de Souza, V.C. de Oliveira Souza, F. Barbosa, Methylmercury and inorganic mercury determination in blood by using liquid chromatography with inductively coupled plasma mass spectrometry and a fast sample preparation procedure, Talanta 80 (2010) 1158–1163, https://doi.org/10.1016/j.talanta.2009.09.001.

[9] Y.S. Hong, E. Rifkin, E.J. Bouwer, Combination of diffusive gradient in a thin film probe and IC-ICP-MS for the simultaneous determination of CH_3Hg^+ and Hg^{2+} in oxic water, Environ. Sci. Technol. 45 (2011) 6429–6436, https://doi.org/10.1021/es200398d.

[10] H. Wang, B. Chen, S. Zhu, X. Yu, M. He, B. Hu, Chip-based magnetic solid-phase microextraction online coupled with MicroHPLC-ICPMS for the determination of mercury species in cells, Anal. Chem. 88 (2016) 796–802, https://doi.org/10.1021/acs.analchem.5b03130.

[11] H.Z. Mousavi, A. Asghari, H.J. Shirkhanloo, Determination of Hg in water and wastewater samples by CV-AAS following on-line preconcentration with silver trap, Anal. Chem. 65 (2010) 935–939, https://doi.org/10.1134/S106193481009008X.

[12] R. Liang, Q. Wang, W. Qin, Highly sensitive potentiometric sensor for detection of mercury in Cl⁻rich samples, Sensor. Actuat. B-Chem. 208 (2015) 267–272, https://doi.org/10.1016/j.snb.2014.11.040.

[13] G. Aragay, J. Pons, A. Merkoi, Enhanced electrochemical detection of heavy metals at heated graphite nanoparticle-based screen-printed electrodes, J. Mater. Chem. 21 (2011) 4326–4331, https://doi.org/10.1039/c0jm03751f.

[14] X. Niu, H. Zhao, M. Lan, Disposable screen-printed bismuth electrode modified with multi-walled carbon nanotubes for electrochemical stripping measurements, Anal. Sci. 27 (2011) 1237–1241, https://doi.org/10.2116/analsci.27.1237.

[15] F. Karimi, M. Alizadeh, A.L. Sanati, Electrochemical sensors, a bright future in the fabrication of portable kits in analytical systems, Chem. Rec. 27 (2020) 682–692, https://doi.org/10.1002/tcr.201900092.

[16] H.K. Maleh, F. Karimi, S. Malekmohammadi, N. Zakariae, R. Esmaeili, S. Rostamnia, M.L. Yola, N. Atar, S. Movaghgharnezhad, S. Rajendran, Am Razmjou, Y. Orooji, S. Agarwal, V.K. Gupta, An amplified voltammetric sensor based on platinum nanoparticle/polyoxometalate/two-dimensional hexagonal boron nitride nanosheets composite and ionic liquid for determination of N-hydroxysuccinimide in water samples, J. Mol. Liq. 310 (2020) 113185, https://doi.org/10.1016/j.molliq.2020.113185.

[17] H.K. Maleh, K. Cellat, K. Arikan, A. Savk, F. Karimi, F. Sen, Palladium–nickel nanoparticles decorated on functionalized-MWCNT for high precision non-enzymatic glucose sensing, Mater. Chem. Phys. 250 (2020) 123042, https://doi.org/10.1016/j.matchemphys.2020.123042.

[18] H.K. Maleh, F. Karimi, Y. Orooji, G. Mansouri, A. Razmjou, A. Aygun, F. Sen, A new nickel-based co-crystal complex electrocatalyst amplified by NiO dope Pt nanostructure hybrid; a highly sensitive approach for determination of cysteamine in the presence of serotonin, Sci. Rep. 10 (2020) 11699, https://doi.org/10.1038/s41598-020-68663-2.

[19] M.G. Motlagh, M, Baghayeri, determination of trace Tl(I) by differential pulse anodic stripping voltammetry using a novel modified carbon paste electrode, J. Electrochem. Soc. 167 (2020), 066508, https://doi.org/10.1149/1945-7111/ab823c.

[20] M. Nodehi, M. Baghayeri, R. Ansari, H. Veisi, Electrochemical quantification of 17α – Ethinylestradiol in biological samples using a au/Fe₃O₄@TA/MWNT/GCE sensor, Mater. Chem. Phys. 244 (2020) 122687, https://doi.org/10.1016/j.matchemphys.2020.122687.

[21] M. Rouhi, M.M. Lakourai, M. Baghayeri, Low band gap conductive copolymer of thiophene with p-phenylenediamine and its magnetic nanocomposite: synthesis, characterization and biosensing activity, Polym. Compos. 40 (2019) 1034–1042, https://doi.org/10.1002/pc.24790.

[22] M. Ghanei-Motlagh, M.A. Taher, M. Fayazi, M. Baghayeri, A. Hosseinifar, Nonenzymatic amperometric sensing of hydrogen peroxide based on vanadium pentoxide nanostructures, J. Electrochem. Soc. 166 (2019) B367–B372, https://doi.org/10.1149/2.0521906jes.

[23] M. Baghayeri, R. Ansari, M. Nodehi, I. Razavipanah, H. Veisi, Label-free electrochemical bisphenol A aptasensor based on designing and fabrication of a magnetic gold nanocomposite, Electroanal. 30 (2018) 2160–2166, https://doi.org/10.1002/elan.201800158.

[24] M. Baghayeri, R. Ansari, M. Nodehi, I. Razavipanah, H. Veisi, Voltammetric aptasensor for bisphenol A based on the use of a MWCNT/Fe3O4@gold nanocomposite, Microchim. Acta 185 (2018) 320, https://doi.org/10.1007/s00604-018-2838-y.

[25] M. Baghayeri, R. Ansari, M. Nodehi, H. Veisi, Designing and fabrication of a novel gold nanocomposite structure: application in electrochemical sensing of bisphenol a, Int. J. Environ. Anal. Chem. 98 (2018) 874–888, https://doi.org/10.1080/03067319.2018.1512595.

[26] P.E. Lokhande, U.S. Chavan, Nanostructured Ni(OH)2/rGO composite chemically deposited on Ni foam for high performance of supercapacitor applications, Mater. Sci. Energy Technol. 2 (2019) 52–56, https://doi.org/10.1016/j.mset.2018.10.003.

[27] S. Ravichandran, E. Karthikeyan, Microwave synthesis-a potential tool for green chemistry, Int. J. ChemTech Res. 3 (2011) 466–470 Corpus ID: 212526048.

[28] R.Z.A. Raja Jamaluddin, Y.H. Lee, L.L. Tan, K.F. Chong, Electrochemical biosensor for nitrite based on polyacrylic-graphene composite film with covalently immobilized hemoglobin, Sensors 18 (2018) 1–17, https://doi.org/10.3390/s18051343.

[29] J. Zhang, F. Zhang, H. Yang, X. Huang, H. Liu, J. Zhang, S. Gup, Graphene oxide as a matrix for enzyme immobilization, Langmuir Lett. 26 (2010) 6083–6085, https://doi.org/10.1021/la904014z.

[30] H.K. Maleh, O.A. Arotiba, Simultaneous determination of cholesterol, ascorbic acid and uric acid as three essential biological compounds at a carbon paste electrode modified with copper oxide decorated reduced graphene oxide nanocomposite and ionic liquid, J. Colloid Interface Sci. 560 (2020) 208–212, https://doi.org/10.1016/j.jcis.2019.10.007.

[31] M. Baghayeri, M.G. Motlagh, R. Tayebee, M. Fayazi, F. Narenji, Application of graphene/zinc-based metal-organic framework nanocomposite for electrochemical sensing of as(III) in water resources, Anal. Chim. Acta 1099 (2020) 60–67, https://doi.org/10.1016/j.aca.2019.11.045.

[32] X. Wu, F. Mu, Y. Wang, H. Zhao, Graphene and graphene-based nanomaterials for DNA detection: a review, Molecules 23 (2018) 2050, https://doi.org/10.3390/molecules23082050.

[33] C.M.L. Carvalho, J. Lu, X. Zhang, E.S.J. Arnér, A. Holmgren, Effects of selenite and chelating agents on mammalian thioredoxin reductase inhibited by mercury: implications for treatment of mercury poisoning, FASEB J. 25 (2011) 370–381, https://doi.org/10.1096/fj.10-157594.

[34] M. Vonlanthen, C.M. Connelly, A. Deiters, A. Linden, N.S.J. Finney, Thiourea-based fluorescent chemosensors for aqueous metal ion detection and cellular imaging, J. Organomet. Chem. 13 (2014) 6054–6060, https://doi.org/10.1021/jo500710g.

[35] S.K. Tripathy, J.Y. Woo, C.S. Han, Colorimetric detection of Fe(III) ions using label-free gold nanoparticles and acidic thiourea mixture, Sensor. Actuat. B-Chem. 181 (2013) 114–118, https://doi.org/10.1016/j.snb.2013.01.058.

[36] W.S. Hummers, R.E. Offeman, Preparation of graphitic oxide, J. Am. Chem. Soc. 80 (1958) 1339, https://doi.org/10.1021/ja01539a017.

[37] N.I. Kovtyukhova, P.J. Ollivier, B.R. Martin, T.E. Mallouk, S.A. Chizhik, E.V. Buzaneva, A.D. Gorchinskiy, Layer-by-layer assembly of ultrathin composite films from microsized graphite oxide sheets and polycations, Chem. Mater. 11 (1999) 771–778, https://doi.org/10.1021/cm981085u.

[38] S. Park, R.S. Ruoff, Chemical methods for the production of graphenes, Nat. Nanotechnol. 4 (2009) 217–224, https://doi.org/10.1038/nnano.2009.58.

[39] H. Misral, S. Sapari, T. Rahman, N. Ibrahim, B.M. Yamin, S.A.J. Hasbullah, Evaluation of novel N -(Dibenzylcarbamothioyl)benzamide derivatives as antibacterial agents by using DFT and drug-likeness assessment, J. Chemother. (2018) 1–5, https://doi.org/10.1155/2018/9176280.

[40] I. Fakhar, N.J. Hussien, S. Sapari, A.H. Bloh, S. Fairus, M. Yusoff, S.A. Hasbullah, Synthesis, X-ray diffraction, theoretical and anti-bacterial studies of bis-thiourea secondary amine, J. Mol. Struct. 1159 (2018) 96–102, https://doi.org/10.1016/j.molstruc.2018.01.032.

[41] G. Bharath, R. Madhu, S.M. Chen, V. Veeramani, A. Balamurugan, D. Mangalaraj, C. Viswanathan, Enzymatic electrochemical glucose biosensors by mesoporous 1D hydroxyapatite-on-2D reduced graphene oxide, J. Mater. Chem. B 3 (2015) 1360–1370, https://doi.org/10.1039/c4tb01651c.

[42] W. Qin, T. Chen, T. Lu, D.H. Chua, L. Pan, Layered nickel sulfide-reduced graphene oxide composites synthesized via microwave-assisted method as high performance anode materials of sodium-ion batteries, J. Power Sources 302 (2016) 202–209, https://doi.org/10.1016/j.jpowsour.2015.10.064.

[43] C.R. Minitha, M. Lalitha, Y.L. Jeyachandran, L. Senthilkumar, R.T. Rajendra Kumar, Adsorption behaviour of reduced graphene oxide towards cationic and anionic dyes: co-action of electrostatic and π – π interactions, Mater. Chem. Phys. 194 (2017) 243–252, https://doi.org/10.1016/j.matchemphys.2017.03.048.

[44] H. Yan, H. Wu, K. Li, Y. Wang, X. Tao, H. Yang, A. Li, R. Cheng, Influence of the surface structure of graphene oxide on the adsorption of aromatic organic compounds from water, ACS Appl. Mater. Interfaces 7 (2015) 6690–6697, https://doi.org/10.1021/acsami.5b00053.

[45] N.H.A. Razak, L.L. Tan, S.A. Hasbullah, Y.H. Lee, Reflectance chemosensor based on bis-thiourea derivative as ionophore for copper(II) ion detection, Microchem. J. 153 (2020) 104460, https://doi.org/10.1016/j.microc.2019.104460.

[46] I. Fakhar, B.M. Yamin, S.A. Hasbullah, A comparative study of the metal binding behavior of alanine based bis-thiourea isomers, Chem. Cent. J. 11 (2017) 76, https://doi.org/10.1186/s13065-017-0304-2.

[47] G. Sun, L. Zhang, Y. Zhang, H. Yang, C. Ma, S. Ge, M. Yan, J. Yu, Z. Song, Multiplexed enzyme-free electrochemical immunosensor based on ZnO nanorods modified reduced graphene oxide-paper electrode and silver deposition-induced signal amplification strategy, Biosens. Bioelectron. 71 (2015) 30–36, https://doi.org/10.1016/j.bios.2015.04.007.

[48] D.A. Skoog, F.J. Holler, S.R. Crouch, Principles of Instrumental Analysis, Sixth ed. Thomson, USA, 2018.

[49] M. Breton, M. Bessodes, S. Bouaziz, J. Herscovici, D. Scherman, N. Mignet, Iminothiol/thiourea tautomeric equilibrium in thiourea lipids impacts DNA compaction by inducing a cationic nucleation for complex assembly, Biophys. Chem. 145 (2009) 7–16, https://doi.org/10.1016/j.bpc.2009.08.003.

[50] F. Fu, Q. Wang, Removal of heavy metal ions from wastewaters: a review, J. Environ. Manag. 92 (2011) 407–418, https://doi.org/10.1016/j.jenvman.2010.11.011.

[51] F.F. Farah, L.L. Tan, S.I. Zubairi, Bienzymatic creatine biosensor based on reflectance measurement for real-time monitoring of fish freshness, Sensor. Actuat. B-Chem. 269 (2018) 36–45, https://doi.org/10.1016/j.snb.2018.04.141.

[52] National Water Quality Standards For Malaysia2006 70–72.

[53] D. Kolodynska, Application of a new generation of complexing agents in removal of heavy metal ions from different wastes, Environ. Sci. Pollut. Res. Int. 20 (2013) 5939–5949, https://doi.org/10.1007/s11356-013-1576-2.

[54] W. Huang, C. Yang, S. Zhang, Anodic stripping voltammetric determination of mercury by use of a sodium montmorillonite-modified carbon-paste electrode, Anal. Bioanal. Chem. 374 (2002) 998–1001, https://doi.org/10.1007/s00216-002-1438-0.

[55] P. Ugo, L.M. Moretto, P. Bertoncello, J. Wang, Determination of trace mercury in saltwaters at screen-printed electrodes modified with sumichelate Q10R, Electroanal. 10 (1998) 1017–1021, https://doi.org/10.1002/(SICI)1521-4109(199810)10:15<1017:: AID-ELAN1017>3.0.CO;2-D.

[56] S. Cinti, F. Santella, D. Moscone, F. Arduini, Hg^{2+} detection using a disposable and miniaturized screen-printed electrode modified with nanocomposite carbon black and gold nanoparticles, Environ. Sci. Pollut. Res. 23 (2016) 8192–8199, https://doi.org/10. 1007/s11356-016-6118-2.

[57] F. Arduini, C. Majorani, A. Amine, D. Moscone, G. Palleschi, Hg^{2+} detection by measuring thiol groups with a highly sensitive screen-printed electrode modified with a nanostructured carbon black film, Electrochim. Acta 56 (2011) 4209–4215, https://doi.org/ 10.1016/j.electacta.2011.01.094.

[58] F.A.A. Ngah, E.I. Zakariah, I. Fakhar, N.I. Hassan, Y.H. Lee, B. Yamin, S.A. Hasbullah, A new thiourea compound as potential ionophore for metal ion sensor, Indones J. Chem. 18 (2018) 116, https://doi.org/10.22146/ijc.27078.

[59] X. Zhou, X. Wang, B. Wang, Z. Chen, C. He, Y. Wu, Preparation, characterization and NH3-sensing properties of reduced graphene oxide/copper phthalocyanine hybrid material, Sensor. Actuat. B-Chem. 193 (2014) 340–348, https://doi.org/10.1016/j.snb. 2013.11.090.